Retinal Expression of *Fgf2* in RCS Rats with Subretinal Microphotodiode Array

Vincent T. Ciavatta,[1,2] *Moon Kim,*[1] *Paul Wong,*[2] *John M. Nickerson,*[2] *R. Keith Shuler, Jr,*[2] *George Y. McLean,*[3] *and Machelle T. Pardue*[1,2]

Purpose. To test the hypothesis that subretinal electrical stimulation from a microphotodiode array (MPA) exerts a neuroprotective effect in Royal College of Surgeons (RCS) rats through the induction of growth factors.

Methods. At postnatal day 21, RCS rats were divided into four groups in which one eye per rat received treatment: (A) active MPA, (M) minimally active MPA, (S) sham surgery, or (C) no surgery and the opposite eye was unoperated. Dark- and light-adapted ERGs were recorded 1 week after surgery. A second set of A-, M-, and C-treated RCS rats had weekly ERG recordings for 4 weeks. Real-time RT-PCR was used to measure relative expression of mRNAs (*Bdnf*, *Fgf2*, *Fgf1*, *Cntf*, *Gdnf*, and *Igf1*) in retina samples collected 2 days after the final ERG.

Results. One week after surgery, there was a slight difference in dark-adapted ERG b-wave at the brightest flash intensity. Mean retinal *Fgf2* expression in the treated eye relative to the opposite eye was greater for the A group (4.67 ± 0.72) than for the M group (2.80 ± 0.45; $P = 0.0501$), S group (2.03 ± 0.45; $P < 0.01$), and C group (1.30 ± 0.22; $P < 0.001$). No significant change was detected for *Bdnf*, *Cntf*, *Fgf1*, *Gdnf*, and *Igf1*. Four weeks after surgery, the A group had significantly larger dark- and light-adapted ERG b-waves than for the M and C groups ($P < 0.01$). Simultaneously, mean relative *Fgf2* expression was again greater for the A group (3.28 ± 0.61) than for the M (1.28 ± 0.32; $P < 0.05$) and C (1.05 ± 0.04; $P < 0.05$) groups.

Conclusions. The results show subretinal implantation of an MPA induces selective expression of *Fgf2* above that expected from a retina-piercing injury. Preservation of ERG b-wave amplitude 4 weeks after implantation is accompanied by elevated *Fgf2* expression. These results suggest that *Fgf2* may play a role in the neuroprotection provided by subretinal electrical stimulation. (*Invest Ophthalmol Vis Sci.* 2009;50:4523–4530) DOI:10.1167/iovs.08-2072

From the [1]Rehab R&D Center, Atlanta VA Medical Center, Decatur, Georgia; the [2]Department of Ophthalmology, Emory School of Medicine, Atlanta, Georgia; and [3]Optobionics Corp., Palo Alto, California.

Supported by the Department of Veterans Affairs, Foundation Fighting Blindness, Research to Prevent Blindness, and National Eye Institute Grants R01EY016470, R24EY017045, and P30EY0636.

Submitted for publication March 25, 2008; revised October 17, 2008, and January 8, 2009; accepted August 5, 2009.

Disclosure: **V.T. Ciavatta**, Optobionics Corp. (F); **M. Kim**, None; **P. Wong**, None; **J.M. Nickerson**, None; **R.K. Shuler, Jr**, None; **G.Y. McLean**, Optobionics Corp. (E, P); **M.T. Pardue**, Optobionics Corp. (F)

The publication costs of this article were defrayed in part by page charge payment. This article must therefore be marked "*advertisement*" in accordance with 18 U.S.C. §1734 solely to indicate this fact.

Corresponding author: Vincent T. Ciavatta, Research Service (151 Oph), 1670 Clairmont Road, Decatur, GA 30033; vciavat@emory.edu.

Retinal degenerations such as age-related macular degeneration (AMD) and retinitis pigmentosa are a significant health concern. Retinitis pigmentosa (RP) occurs in approximately 1 in 3500 persons.[1] As of 2003, AMD affected an estimated 20 to 25 million persons worldwide, and the incidence of AMD is projected to triple in 30 to 40 years.[2] A multitude of mutations and risk factors underlie the mechanisms of RP[3] and AMD[4–7]; however, all forms of these retinal degenerations result in irreversible photoreceptor cell death and thus visual impairment or blindness.[8]

For patients with RP and AMD, neuroprotective strategies aim to prevent or delay irreversible photoreceptor death and thereby prolong useful vision. A variety of neuroprotective approaches including growth factor administration,[9] antioxidant combination therapy,[10,11] steroids,[12] bile acids,[13] and calcium-channel blockers[14] have been shown to extend neuroprotection to photoreceptors in animal models of retinal degeneration. Administering growth factors to eyes of such animal models through direct injection,[15] encapsulated, engineered ciliary neurotrophic growth factor (CNTF)-secreting cells,[16] or transfection with a growth factor–encoding vector[17] is well documented to protect the retina from some diseases or injury. Similarly, inducing the expression of endogenous growth factor genes through trauma to the eye[18] also provides neuroprotection in the retinas of rodent models of retinal degeneration.

Electrical stimulation may also be capable of exerting a neuroprotective effect on retinal neurons. Patients with RP who, as part of a clinical trial, received a microphotodiode array implanted into the subretinal space of one eye displayed measurable increases in visual acuity and color vision.[19] Eyes of Royal College of Surgeons (RCS) rats implanted with subretinal microphotodiode arrays (MPAs) similar to those used in human trials showed a delay in the loss of photoreceptor function as determined by electroretinogram (ERG) b-wave amplitude and higher photoreceptor counts near the implantation site compared with control eyes.[20] RCS rats receiving transcorneal electrical stimulation also experienced a delay in photoreceptor death, preservation of retinal thickness, and preservation of retinal function.[21] Lastly, in rats with a transected optic nerve, transcorneal electrical stimulation spared axotomized ganglion cells.[22]

In nonretinal neurons, electrical stimulation has been associated with neuroprotection. For example, electrical stimulation of spiral ganglion cells after a deafening stress[23] and the cerebellar fastigial nucleus before midcerebral artery occlusion[24] resulted in prolonged neuron survival. Electrical stimulation has been associated with neuroprotection of dopaminergic neurons in a rat model of Parkinson disease.[25]

Electrical stimulation has been shown to induce neuronal expression of neuroprotective growth factors in culture[26–28] and in vivo.[29–31] Some of these studies also showed that growth factor induction in response to electrical stimulation was associated with neuroprotective effects.[21,27–30] Further-

more, a causal relationship between electrical stimulation, *Igf1* induction, and neuroprotection of axotomized ganglion cells was established when ganglion cell rescue by transcorneal electrical stimulation was abrogated by an IGF-1 receptor antagonist.[32] Thus, it seems plausible that the induction of a neuroprotective growth factor is responsible, at least in part, for the preservation of retinal function and photoreceptors in RCS rats that received subretinal electrical stimulation.[20]

We hypothesized that neuroprotection of the RCS rat retina in response to subretinal electrical stimulation[33] results from heightened activity of neuronal survival pathways that are activated by growth factors. We therefore predicted that transcript levels of neuroprotective growth factors would be elevated in RCS rats that received subretinal electrical stimulation from MPAs. Here we report the expression of several growth factors (brain-derived neurotrophic factor [*Bdnf*], ciliary neurotrophic factor [*Cntf*], acidic fibroblast growth factor [*Fgf1*], basic fibroblast growth factor [*Fgf2*], glial-derived neurotrophic factor [*Gdnf*], and insulin-like growth factor [*Igf1*]) in RCS rats that received subretinal electrical stimulation from an active MPA (A), minimally active MPA (M), sham surgery (S), or no treatment control (C). One week after implantation surgery, *Fgf2* expression was selectively induced compared with the other growth factors, with an increasing gradient of expression from the C group, to the S group, to the M group, to the highest expression in the A group. Four weeks after surgery, *Fgf2* expression was still greatest in the A group. Additionally, at 4 weeks after surgery, ERG b-wave amplitudes were significantly larger in the A group than in the other treatment groups. These results suggest that *Fgf2* induction may mediate neuroprotective effects from subretinal electrical stimulation.

METHODS

Animals, Surgical Procedures, and Experimental Design

The dystrophic RCS rat retinal degeneration model, originally obtained from Matthew LaVail, PhD, of the University of California at San Francisco, was used in this study. The mutation was bred onto the Long Evans background; thus, pigmented animals were used throughout this study. In the dystrophic RCS rat, both copies of the receptor tyrosine kinase gene *Mertk* are mutated, resulting in a premature stop codon and improper protein synthesis.[34] The lack of the MERTK enzyme prohibits the phagocytosis of photoreceptor outer segments[35] and is believed to be the cause of the photoreceptor degeneration that begins at approximately postnatal day (P) 12 and is complete by approximately P95.[36] Animals were reared and maintained throughout the study on a 12-hour light (~100 lux)/12-hour dark schedule and were provided food and water ad libitum.

Electrical stimulation was provided by a subretinally implanted MPA that has been described previously.[37,38] To control for potential neuroprotective effects from injury[18] or light exposure,[39] animals were divided into four treatment groups: nonsurgical control (C; $n = 11$), sham surgery (S; $n = 9$), minimally active MPA implantation (M; $n = 10$), and active MPA implantation (A; $n = 19$). At P21, surgeries were performed as described previously.[40] For A and M treatments, implants remained in the subretinal space for the duration of the study, whereas the S treatment involved inserting the MPA into the subretinal space and immediately removing it. One week (7 days) after implantation, 8, 9, 6, and 14 animals in the C, S, M, and A groups, respectively, were subjected to ERG and then humanely killed 2 days later (9 days after implantation). All other animals were monitored with weekly ERGs to 4 weeks (28 days) after implantation surgery and then humanely killed 2 days after the final ERG (30 days after implantation). Animal kill was performed with an overdose of pentobarbital. All experiments involving animals were reviewed and approved by the Institutional Animal Care and Use Committee of the Atlanta Veterans Administration and were in full compliance with the ARVO Statement for the Use of Animals in Ophthalmic and Visual Research.

Electroretinographic Assessment of Retinal Function

ERGs were recorded under dark- and light-adapted conditions, as previously described.[20] Briefly, rats were dark-adapted overnight and prepared under dim red light. After sedation with ketamine (60 mg/kg) and xylazine (7.5 mg/kg), the cornea was anesthetized (1.0% tetracaine), and dilating drops (1.0% tropicamide, 1% cyclopentolate) were instilled in both eyes. With body temperature maintained at 37°C on a homeothermic heating pad, the electrical response of the retina was recorded with a nylon fiber embedded with silver particles placed across the surface of the cornea[41] and wetted with 1% methylcellulose. Responses were referenced and grounded by needle electrodes placed in the cheek and tail, respectively. A series of full-field flash stimuli was presented by a Ganzfeld dome under dark-adapted conditions (−3.4 to 2.1 log cd · s/m^2). Interflash interval increased with flash intensity from 10 to 60 seconds. After 10 minutes of light adaptation (30 cd/m^2), a second series of flash stimuli (−0.82 to 1.88 log cd · s/m^2) was presented in the presence of the adapting light at 2.1 Hz to isolate cone responses. Acquired responses were filtered (1–1500 Hz) and stored on a commercial ERG system (UTAS 3000; LKC Technologies, Gaithersburg, MD). ERG recordings performed 1 week after surgery consisted of five dark-adapted and four light-adapted steps. Weekly ERG recordings of rats followed to 4 weeks after surgery served to measure retinal function and to provide increased electrical output from the MPA,[33] thus consisting of 10 dark-adapted and 7 light-adapted steps.

Implant Description and Characterization

Implants were fabricated essentially as described previously.[38] Briefly, active MPAs were made from p-type starting material and contained an array of pixels consisting of n-type doped regions on the front (pixilated) surface. In contrast, the minimally active MPAs were made without the intentional introduction of any additional dopants, so the minimally active MPAs were not expected to have any semiconductor junctions or to exhibit photovoltaic behavior. The minimally active MPAs were manufactured from p-type monocrystalline silicon wafers with a resistivity of 50 Ω cm. The starting material was polished on both sides and selectively thinned (by wet etching in KOH) to form membranes 23 μm thick. A dielectric layer of silicon dioxide was formed by dry thermal oxidation of the silicon. The resultant dielectric layer was 1200 ± 50 Å thick and covered both sides of each MPA. Implantable discs were cut from the thin portions of the wafer by etching annuli completely through the 23-μm membranes using a reactive ion etch process. No metal electrodes were applied to the minimally active MPAs, so each face consisted of a smooth, continuous layer of silicon dioxide.

The photovoltaic charge-injection characteristics (μA/cm^2/W) of active and minimally active MPAs were measured in a PBS electrolyte under a wide range of illumination conditions using an infrared source (870 nm). A pulse (1 ms) of light (10.5 mW/cm^2) was shown on the photoactive side of the active MPAs or either side of the minimally active MPAs as current was monitored in the PBS electrolyte at one measurement every 10^{-4} seconds.

Growth Factor Expression Analysis

Before enucleation, the superior portion of each eye was marked with a pen to maintain orientation. Eyes were enucleated, cornea and lens were removed, and four radial cuts were made to flatten the eyecup. A 2.3-mm diameter trephine was used to dissect the portion of retina overlying the implant (A and M groups), the incision site (S group), or an equivalent position (C group).

For each tissue sample, reverse transcription (RT) followed by real-time polymerase chain reaction (PCR) was performed. Samples were homogenized in 100 μL reagent (TRIzol; Invitrogen, Carlsbad, CA) at 30,000 rpm for 2 × 15 seconds using a *TH* homogenizer

equipped with a 5-mm stainless steel probe (Omni International, Marietta, GA). Total RNA isolation was performed according to the manufacturer's instructions. Resultant RNA was dissolved in 100 μL RNase-free dH_2O and further purified and concentrated to a final volume of 12 μL with a spin column (MinElute RNeasy; Qiagen, Valencia, CA). RNA yields, as determined by measuring A_{260} nm, varied between approximately 0.5 and 2.0 μg per sample, and the ratios of A_{260} nm to A_{280} nm varied between 1.7 and 2.0.

Optimal RNA and cDNA dilutions were determined by RT and subsequent PCRs on a seven-step, twofold dilution series of RNA (12.5, 25, 50, 100, 200, 400, and 800 ng RNA/RT) and inspecting for single cycle shifts in cycle threshold (Ct) between dilutions. Using more than 200 ng RNA per RT decreased 18S Ct differences, implying incomplete RT of 18S at high RNA amounts, and using less than 50 ng RNA per RT increased Ct for genes of interest. For each RNA sample, 100 ng total RNA was reverse transcribed (Quantitect Reverse Transcriptase; Qiagen) in a final 20-μL volume according to the manufacturer's instructions. The resultant cDNA was diluted 20-fold, and 5 μL diluted cDNA (equivalent of 1.25 ng RNA/PCR) was used in a real-time PCR reaction with 100 nM (*Fgf1* and *Gdnf*) or 200 nM (*18S*, *Bdnf*, *Cntf*, *Fgf2*, *Igf1*) each of a primer pair (*18S* forward, 5′-GTTGGTTTTCGGAACTGAGGC-3′, *18S* reverse, 5′-GTCGGCATCGTTTATGGTCG-3′; *Bdnf* forward, 5′-AACCAGAAAAAGCACCAAAA-3′, *Bdnf* reverse, 5′- CTTGTGCTGAATGGACAGAA-3′; *Cntf* forward, 5′-GGACCTCTGTAGCCGTTCTA-3′, *Cntf* reverse, 5′-TCATCTCACTCCAACGATCA-3′; *Fgf1* forward, 5′-AACCCAAACTGCTCTACTGC-3′, *Fgf1* reverse, 5′- GAGCCGTATAAAAGCCCTTC-3′; *Fgf2* forward, 5′-GCGGCTCTACTGCAAGA-3′, *Fgf2* reverse, 5′-CGTCCATCTTCCTTCATAGC-3′; *Gdnf* forward, 5′-CCATGTTCCTAGCCACTCTG-3′, *Gdnf* reverse, 5′- AGGCTGAAGTTGGTTTCCTT-3′; *Igf1* forward, 5′-TGGACGCTCTTCAGTTCGTG-3′, *Igf1* reverse, 5′-GTTTCCTGCACTTCCTCTAC-3′), 12.5 μL of 2× reaction cocktail (iQ SYBR Green Supermix; Bio-Rad, Hercules, CA) and nuclease-free dH_2O to 25 μL. Primers were designed with Primer3 (http://fokker.wi.mit.edu/primer3/).[41] cDNA was amplified in 96-well plates on a thermal cycler (MyIQ; Bio-Rad). Conditions were 95°C, 3 minutes; 40 cycles of 94°C, 30 seconds denaturation; 55°C, 30 seconds annealing; 72°C, 30 seconds extension; 72°C, 7 minutes, with fluorescence recorded at the end of each 72°C extension. Melt analysis conditions were heating from 55°C to 95°C in 0.5°C increments, 15 seconds per increment, with fluorescence recorded at each increment. The Ct of each reaction was determined from a PCR baseline-subtracted and curve-fit option (iCycler; Bio-Rad). Three real-time PCRs were performed for each cDNA sample-primer pair combination, and the average Ct was calculated. Taking 18S as the endogenous control, growth factor transcript abundance (expression) relative to control eyes or the opposite eye was calculated from the average PCR cycle thresholds using the $2^{-\Delta\Delta Ct}$ method of Livak and Schmittgen.[42] The expression ratio was computed to minimize animal-to-animal variability in gene expression.

Statistical Analysis

For replicate analyses of treatment groups, the mean and SEM were calculated. Preliminary growth factor expression data were analyzed for significance with Student's *t*-test. One-way (*Fgf2* expression) and two-way (ERG a- and b-wave amplitudes) analysis of variance tests were performed to determine whether there were significant differences within all treatment groups, and the Holm-Sidak post hoc test was applied to examine significant differences between two treatment groups at $\alpha = 0.05$ with the use of statistical analysis software (SigmaStat 3.5; Systat Software, Inc., Point Richmond, CA).

Results

Implant Characterization

Minimally active MPAs exhibited a photovoltaic effect, suggesting that a photoactive junction was inadvertently formed during their manufacture. At all illumination levels, however, the active MPAs delivered more charge than the minimally active MPAs. Figure 1 shows that the active MPA delivered greater than 100 times more stimulus current than the minimally active MPA in response to illumination of approximately 10 mW/cm^2 of near infrared (870 nm) light. At this wavelength, the MPA had a responsivity of 0.345 A/W (see Fig. 1 in DeMarco et al.[44]) and responded in a linear fashion to increasing light intensity. Thus, the difference was less pronounced at lower illumination levels and more pronounced at greater illumination levels because the charge capacity of the iridium oxide electrodes on the active MPAs far exceeded the small capacitive coupling available to the minimally active MPAs. Because lighting conditions used during the study ranged from darkness to the brightest ERG flash (2.1 log cd · s/m^2) with the large fluctuations between these extremes, it is estimated that retinas in the A group experienced more than 100 times more current than retinas in the M group.

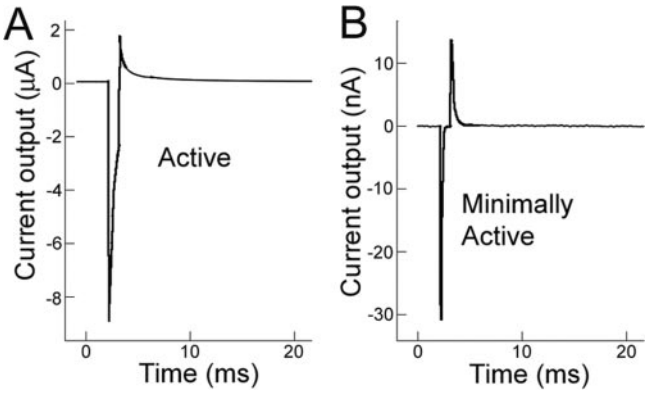

Figure 1. In vitro testing of the active and minimally active microphotodiode arrays. MPAs were placed in PBS and exposed to an 870-nm flash of 10.5-mW/cm^2 intensity and 1-ms duration. The graphs show representative current output of active (**A**) and minimally active (**B**) MPAs from this testing. Note the change in current scale from microamps to nanoamps between (**A**) and (**B**), respectively. The active MPA produces current that is more than two orders of magnitude above that from the minimally active MPA (~8 μA compared with ~30 nA, respectively).

Electroretinographic Assessment of Retinal Function

Dark-Adapted Responses. Representative dark-adapted ERGs from animals at 1 and 4 weeks after surgery are shown in Figure 2. Figure 2A shows the typical ERG waveform to a bright flash (2.1 log cd · s/m^2) from a representative RCS rat in each treatment group at 28 days of age. To this flash intensity, all treatment groups had prominent a- and b-waves with oscillatory potentials present on the leading edge of the b-wave. The negative spike at 0.05 ms was attributed to the electrical activity of the MPA or M-device at light onset and can be seen in each waveform from the A or M group. Figure 2C shows the average intensity response functions for the a- and b-wave at 1 week after implantation from each treatment group. There were no significant differences in the a-wave amplitude. However, the b-wave amplitude was significantly larger in the A and S groups than in the M and C groups at the brightest flash intensity (two-way repeated ANOVA; $P = 0.02$).

After 4 weeks of treatment by the MPA device, there was a significant difference in the overall waveform amplitude of the A group compared with the C and M groups, as shown in Figure 2B. The representative waveforms in Figure 2B show smaller waveforms compared with the 1-week recordings (Fig. 2A), reflecting the progressing photoreceptor degeneration in the RCS rats. Figure 2D shows the average a- and b-wave

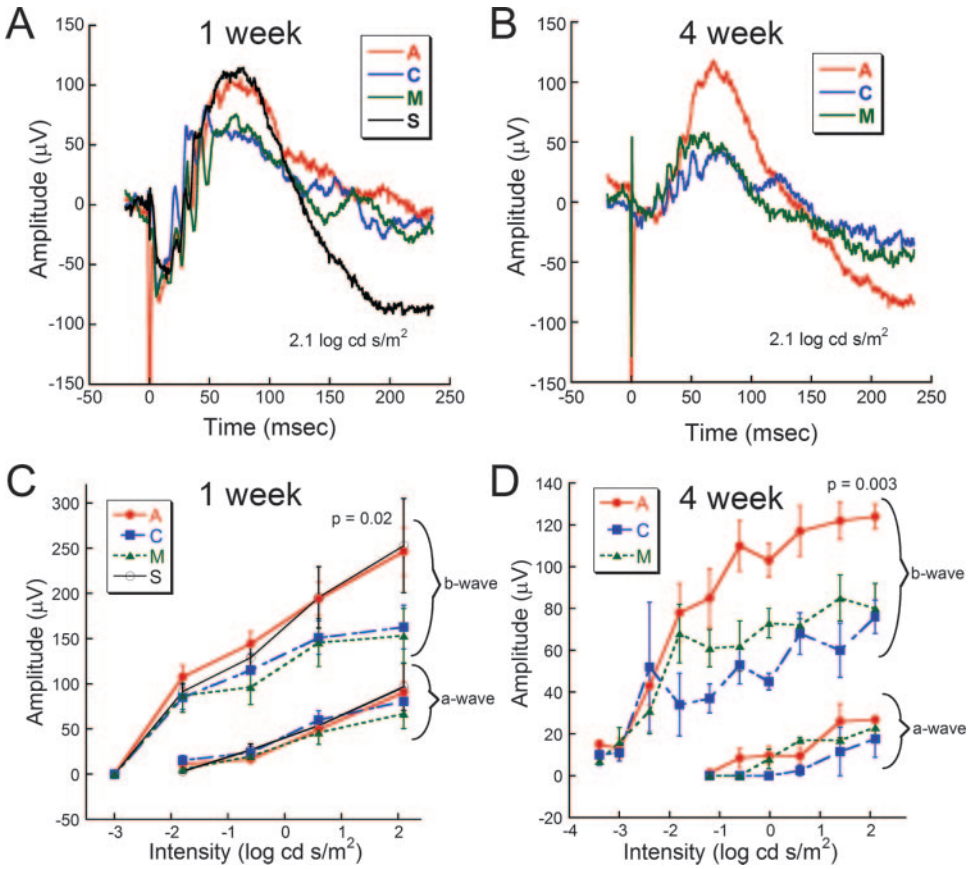

FIGURE 2. Retinal function as assessed by dark-adapted ERG b-wave at 1 and 4 weeks after implantation. (**A**) Representative waveforms from each treatment group in response to a bright flash stimulus (2.1 log cd · s/m^2) at 1 week after implantation. The eyes from the A and S groups have slightly larger b-wave amplitudes than the eyes from the C and M groups. The large negative spike at 0.05 ms reflects the electrical activity of the A and M devices. (**B**) Representative waveforms from the A, C, and M groups at 4 weeks after implantation. The response from the A group is twice as large as the response from the C and M groups. (**C**) Average (±SEM) amplitude of a- and b-waves at 1 week after surgery from A (n = 12), C (n = 9), M (n = 7), and S (n = 7) groups. The b-wave amplitudes of the A and S groups are significantly larger than of the M and S groups at the brightest flash intensity. No differences were found in a-wave amplitudes at this time. (**D**) Average amplitude of a- and b-waves at 4 weeks after surgery from A (n = 5), C (n = 3), and M (n = 4) groups. The b-wave amplitude from the A group is significantly larger than the M and C groups at most intensities. There were no differences in a-wave amplitudes between the groups.

amplitudes across intensity. The A group had a significantly larger b-wave amplitudes in response to intensities greater than −0.6 log cd · s/m^2 (two-way ANOVA; P = 0.003). No significant differences in a-wave amplitude were found between treatment groups.

Light-Adapted Responses. Figure 3 shows cone-isolating, light-adapted responses recorded 1 and 4 weeks after implantation. Note that the loss of cone function in the progressive photoreceptor degeneration can be clearly seen by the decreasing amplitude responses between 1 and 4 weeks (28 and 49 days of age, respectively). Figures 3A and 3C illustrate no significant differences in the light-adapted waveform or average b-wave amplitude, respectively, between treatment groups at 1 week after treatment. However, by 4 weeks after treatment, the A group had significantly larger responses, as shown by the representative waveforms in Figure 3B. The b-wave amplitude in the A group was significantly larger than the C and M groups at intensities greater than 0.39 log cd · s/m^2 (two-way ANOVA, P = 0.003: Fig. 3D).

Growth Factor Expression Analyses by RT-PCR

Nine days after surgery, expression analyses by RT-PCR of *Cntf, Fgf1, Fgf2, Gdnf, Igf1*, and *Bdnf* (not shown) showed a consistent, large, and significant elevation of *Fgf2* expression in the A group compared with all other treatment groups, whereas little to no change across treatment groups was observed for the other genes (Fig. 4). Additional surgeries and 9-day analyses of the *Fgf2* expression ratio again showed significantly elevated *Fgf2* expression in the A group (Fig. 5A) but also revealed an increase as treatment progressed from control to sham to minimally active implantation to active implantation (C, 1.30 ± 0.22; S, 2.03 ± 0.45; M, 2.80 ± 0.45; and A, 4.67 ± 0.72; $F_{3,36}$ = 6.67; P = 0.001). Post hoc Holm-Sidak analysis revealed significant differences between the A and S groups ($P < 0.01$) and the A and C groups ($P < 0.001$), whereas P = 0.0501 for the A to M group comparison.

Thirty days after surgery, *Fgf2* expression was still elevated in the A group (3.24 ± 0.61) compared with the other treatment groups: M, 1.28 ± 0.32; C, 1.05 ± 0.04 ($P < 0.05$, post hoc Holm-Sidak) (Fig. 5B). Over time, *Fgf2* expression in the A group trended lower by 30 days after surgery but was not significantly different from the 9-day level (P = 0.076).

DISCUSSION

Based on known neuroprotective effects of growth factors in various rodent models of retinal degenerative diseases,[9] the induction of growth factors in applications of neuronal electrical stimulation,[27–30] and previous results that indicated some degree of neuroprotection in the retina was provided by retinal electrical stimulation.[19–21,29,45] we hypothesized that electrical stimulation affects neuroprotective pathways by the induction of known neuroprotective growth factors. The present results indeed show an increased expression of *Fgf2* with MPA implantation. As shown previously,[20] MPA implantation in the RCS rat had a positive effect on retinal function 4 weeks after implantation (ERG). Because the active MPA is known to produce approximately 100 times more electric current than the minimally active implant in response to light, it is inferred that the amount of subretinal current was the only difference between rats implanted with the active MPA and rats implanted with the minimally active device. Consequently, the present data imply that subretinal electrical stimulation from the MPA provides neuroprotection to the RCS rat retina concomitant to *Fgf2* induction.

In this study, we began growth factor expression analyses 9 days after MPA implantation even though significant neuroprotection (preservation of maximum ERG b-wave responses and

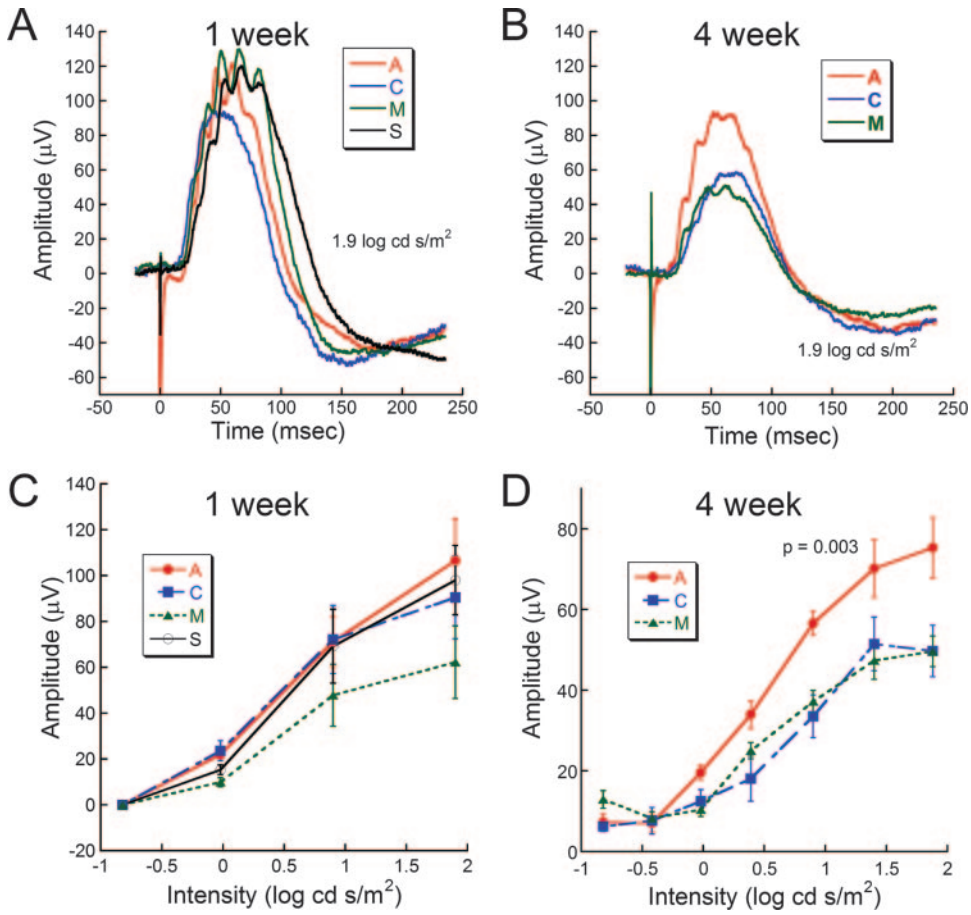

FIGURE 3. Cone function assessed by light-adapted ERGs at 1 week and 4 weeks after implantation. (**A**, **B**) Representative light-adapted waveforms from each treatment group at 1 and 4 weeks after implantation, respectively. Although no differences are observed in the 1-week waveforms, the response from the (**A**) group is approximately 45% larger than the C and M waveforms at 4 weeks after implantation. (**C**) Average light-adapted b-wave amplitude at 1 week after implantation from the A ($n = 12$), C ($n = 9$), M ($n = 7$), and S ($n = 7$) groups showed no differences. (**D**) Average light-adapted b-wave amplitude from the A ($n = 5$), C ($n = 3$), and M ($n = 4$) groups at 4 weeks after implantation showed significantly increased amplitudes in the A group at mid to bright intensities.

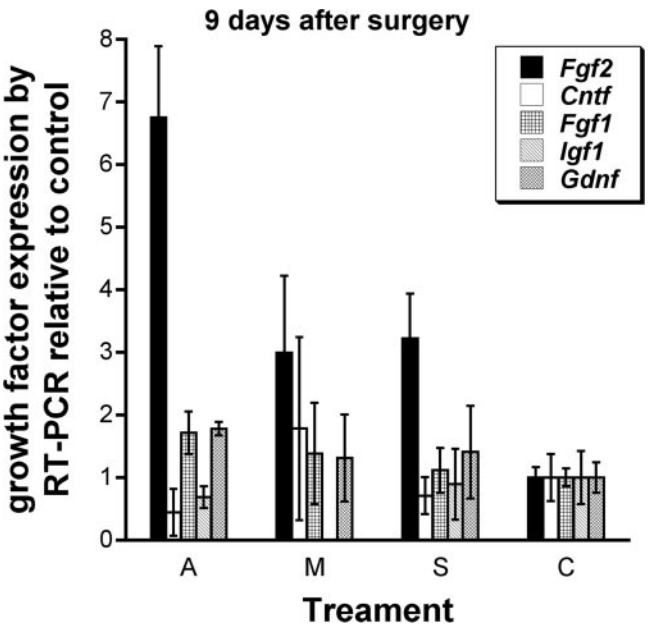

FIGURE 4. Summary of growth factor expression analyses by RT-PCR performed 9 days after surgery. Results are reported as growth factor expression in the treated eye relative to the control eye. *Fgf2* expression in the A group was greater than in all other groups ($P < 0.05$). Number of replicates for A, M, S, and C treatment groups, respectively, were as follows: for *Fgf2*, *Cntf*, and *Fgf1*: 4, 3, 4, and 6; for *Gdnf*: 4, 3, 4, and 5; for *Igf1*: 8, 0, 3, and 10. Error bars are ± SEM.

photoreceptor nuclei) was first noted 4 and 6 weeks after implantation for the A group compared with all other groups.[20] This was based on the expectation that the effects on gene expression would be detectable soon after implantation, in advance of any detectable neuroprotection. For gene expression analysis, we chose to use RT-PCR for its sensitivity and simplicity. We sampled a 2.3-mm diameter piece of retinal tissue centered on the 1-mm diameter implant (or an equivalent location in the nonimplanted eyes) as opposed to sampling the entire retina to optimize detecting any changes in gene expression in retina overlying the implant. Expression analyses at 1 week showed that mean *Fgf2* transcript abundance increased as treatments progressed from no injury (C), to injury (S), to injury plus chronic foreign body plus low level electrical stimulation (M), to injury plus chronic foreign body plus higher level electrical stimulation (A; Fig. 4), whereas little change in mean expression was noted for *Fgf1*, *Cntf*, *Gdnf*, *Igf1*, and *Bdnf*. In addition, *Fgf2* expression at 4 weeks remained elevated in the A group. These data suggest that subretinal electrical stimulation specifically initiated and sustained increased *Fgf2* gene expression.

Fgf2 Induction from Acute Injury and Chronic Electrical Stimulation

As a response to injury alone, *Fgf2* induction was expected and observed. The present results show approximately a twofold increase in mean *Fgf2* expression in the S group compared with the C group. According to published work[46] in which the effect of a retina-piercing injury on growth factor expression was analyzed, detectable *Fgf2* induction might be expected from a retina-piercing injury in a 21-day-old rat with sampling performed 9 days after injury, as shown here (Figs. 4, 5A).

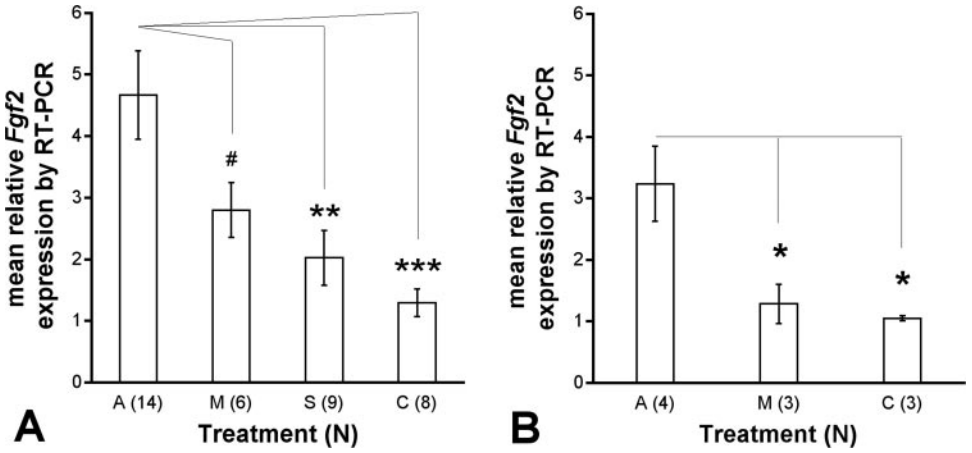

FIGURE 5. *Fgf2* expression analyses by RT-PCR at 9 and 30 days after surgery. Results are reported as *Fgf2* expression in the treated eye relative to the opposite eye at 9 days (**A**) and 30 days (**B**) after surgery. (**A**) Nine days after surgery, *Fgf2* expression tended to increase as treatment progressed from C to S to M to A. (**B**) Thirty days after surgery, *Fgf2* expression remained elevated in the A group compared with the M and C groups. Post hoc Holm-Sidak analysis significance scores were as follows: $\#P = 0.0501$; $^{*}P < 0.05$; $^{**}P < 0.01$; $^{***}P < 0.001$. Error bars are ± SEM.

Similarly, it is not surprising that *Cntf* and *Igf1* induction were not observed with injury at this early age given the small amount of induction (*Cntf*) and decreased expression (*Igf1*) of these genes seen in the injury response studies.[46,47]

Fgf2 expression was induced in electrically stimulated retinas beyond injury-induced levels 1 week after implantation. The A group showed a significant increase in mean *Fgf2* expression (4.7 ± 0.72) compared with the S and C groups (2.03 ± 0.45 and 1.3 ± 0.22) and a noticeable increase in *Fgf2* levels compared with the M group (2.80 ±0.45; $P = 0.0501$). These data may reflect that chronic implantation of a foreign body into the subretinal space, electrical stimulation, or both, induced *Fgf2* beyond sham surgery. If electrical stimulation contributes to *Fgf2* induction in a dose-dependent manner, it might be expected that *Fgf2* expression in the M group would be intermediate between that in the S and A groups because the M group experienced some degree of electrical stimulation, albeit much less than did the A group. Indeed, the 9-day data could be interpreted as showing a dose-response relationship between the charge delivered to the retina and *Fgf2* induction. Data from 30 days after surgery, however, suggest that electrical stimulation is more important for *Fgf2* induction than chronic implantation of the MPA because *Fgf2* remains elevated in the A group, whereas the M group is nearly indistinguishable from the C group. Thus, it appears there is an initial burst of *Fgf2* induction immediately on implantation that could be related to implantation and electrical stimulation, and continued electrical stimulation from the active MPA maintains the induction to at least 30 days after implantation.

The source and mechanism of *Fgf2* induction in response to subretinal electrical stimulation are unknown. However, rat Müller cells are known to be a source of FGF2 in response to various stimuli,[47,48] including an alternating current (1-ms pulses, 20 Hz, 1, 5, and 10 mA, 20 mm between electrodes) that is applied to cultured rat Müller cells.[28] Thus, the Müller cell seems a likely site of *Fgf2* induction in response to electrical stimulation.

The mechanism of induction is less clear. Pharmacologically blocking L-type voltage-dependent calcium channels (VDCCs) has been shown to induce *Fgf2* expression[14] and to delay photoreceptor apoptosis[48] in RCS rats. However, it is not clear whether or how electrical stimulation from the MPA blocks L-type VDCCs. In fact, in vitro induction of *Igf1*[27] and *Bdnf*[26] by electrical stimulation of cultured rat Müller cells was dependent on *functional* L-type VDCCs. Thus, induction of *Fgf2* by identical treatment of cultured rat Müller cells[28] could not have been caused by a block of L-type VDCCs. Nevertheless, this does not rule out the possibility that treatment with the MPA does inactivate L-type VDCCs. Alternatively, given that trauma to the retina is known to induce *Fgf2*, another possible mechanism is recurring trauma from the MPA sufficient to prolong *Fgf2* induction. Future experiments will be directed toward investigating these possibilities.

Relationship between Fgf2 and Retinal Function

As expected from our previous studies, the ERG response did not show a difference 1 week after implantation,[20] whereas *Fgf2* expression was increased. It is not apparent whether the increases in b-wave amplitude at the highest flash intensity for the A and S groups were relevant to neuroprotection because this had not been observed before. By 4 weeks of implantation, the A group showed significantly larger dark-adapted b-wave amplitudes than the other treatment groups, as previously reported.[19] Additionally, the preservation of light-adapted response was also found in the A group at 4 weeks after implantation, suggesting preservation of cone function. Preservation of retinal function at this time point may be a direct result of the selective increase in *Fgf2* expression that promotes a neuroprotective environment. Thus, the current working hypothesis is that electrical stimulation in the A group was capable of achieving a threshold of *Fgf2* induction necessary to elicit neuroprotective effects such as preserved retinal function in degenerating retina. This neuroprotective effect is capable of anatomically preserving photoreceptors, as evidenced by a previous study of RCS rats after 8 weeks of implantation with MPAs.[33] Additional studies, including quantitative analysis of FGF2 protein in response to subretinal electrical stimulation and inhibition of FGF2 signaling, will be required to determine whether the *Fgf2* induction reported here plays a primary or ancillary role in neuroprotection in this model system.

Electrical Stimulation as a Neuroprotective Treatment for Retinal Disease

Neuroprotection in general is a phenomenon with potential clinical applications to treat neurodegenerative diseases. In the eye, growth factors appear to be the most potent of well-tolerated molecules for the neuroprotection of photoreceptors. Specifically, CNTF has been shown to prolong the life of photoreceptors in several different retinal degeneration (RD) animal models, and clinical trials have begun to assess its safety and efficacy to delay the progression of photoreceptor and vision loss in patients with AMD and RP.[49,50] Here we began to explore the mechanism behind neuroprotection provided from a subretinally implanted microphotodiode array. Results suggest that the electrical stimulation induced endogenous *Fgf2*, another growth factor known to exert neuroprotective effects in RD animal models.

Electrical stimulation as a treatment for retinal degeneration could be applied externally or internally. Morimoto et al.[21] also

showed that transcorneal electrical stimulation of RCS rats exerted a neuroprotective effect on photoreceptors. This transcorneal approach requires current to be periodically applied through a contact lens electrode, and it presumably must traverse portions of the cornea and anterior chamber to elicit effects in the retina. Alternatively, a subretinal MPA, though more invasive, has the potential benefits of continuous and precise current delivery to the targeted neurons. The induction of *Igf1* with transcorneal electrical stimulation[21] and *Fgf2* with subretinal electrical stimulation, as shown here, may indicate that growth factor expression may be induced by different stimulation parameters. Irrespective of the mode of delivery, determining whether retinal neuroprotection provided by electrical stimulation can be extended to other RD animal models and determining whether the effects are responsive to stimulation parameters are questions that bear further examination if this approach is to be used as a therapy for human retinal degenerative diseases.

References

1. Haim M. Epidemiology of retinitis pigmentosa in Denmark. *Acta Ophthalmol Scand Suppl.* 2002;1–34.
2. Chopdar A, Chakravarthy U, Verma D. Age related macular degeneration. *BMJ.* 2003;326:485–488.
3. Koenekoop RK, Lopez I, den Hollander AI, Allikmets R, Cremers FP. Genetic testing for retinal dystrophies and dysfunctions: benefits, dilemmas and solutions. *Clin Exp Ophthalmol.* 2007;35:473–485.
4. Klein RJ, Zeiss C, Chew EY, et al. Complement factor H polymorphism in age-related macular degeneration. *Science.* 2005;308:385–389.
5. Rivera A, Fisher SA, Fritsche LG, et al. Hypothetical LOC387715 is a second major susceptibility gene for age-related macular degeneration, contributing independently of complement factor H to disease risk. *Hum Mol Genet.* 2005;14:3227–3236.
6. Yang Z, Camp NJ, Sun H, et al. A variant of the *HTRA1* gene increases susceptibility to age-related macular degeneration. *Science.* 2006;314:992–993.
7. Klein R. Overview of progress in the epidemiology of age-related macular degeneration. *Ophthalmic Epidemiol.* 2007;14:184–187.
8. Wenzel A, Grimm C, Samardzija M, Reme CE. Molecular mechanisms of light-induced photoreceptor apoptosis and neuroprotection for retinal degeneration. *Prog Retin Eye Res.* 2005;24:275–306.
9. LaVail MM, Yasumura D, Matthes MT, et al. Protection of mouse photoreceptors by survival factors in retinal degenerations. *Invest Ophthalmol Vis Sci.* 1998;39:592–602.
10. Komeima K, Rogers BS, Lu L, Campochiaro PA. Antioxidants reduce cone cell death in a model of retinitis pigmentosa. *Proc Natl Acad Sci U S A.* 2006;103:11300–11305.
11. Komeima K, Rogers BS, Campochiaro PA. Antioxidants slow photoreceptor cell death in mouse models of retinitis pigmentosa. *J Cell Physiol.* 2007;213:809–815.
12. Dykens JA, Carroll AK, Wiley S, et al. Photoreceptor preservation in the S334ter model of retinitis pigmentosa by a novel estradiol analog. *Biochem Pharmacol.* 2004;68:1971–1984.
13. Boatright JH, Moring AG, McElroy C, et al. Tool from ancient pharmacopoeia prevents vision loss. *Mol Vis.* 2006;12:1706–1714.
14. Sato M, Ohguro H, Ohguro I, et al. Study of pharmacological effects of nilvadipine on RCS rat retinal degeneration by microarray analysis. *Biochem Biophys Res Commun.* 2003;306:826–831.
15. Faktorovich EG, Steinberg RH, Yasumura D, Matthes MT, LaVail MM. Photoreceptor degeneration in inherited retinal dystrophy delayed by basic fibroblast growth factor. *Nature.* 1990;347:83–86.
16. Tao W, Wen R, Goddard MB, et al. Encapsulated cell-based delivery of CNTF reduces photoreceptor degeneration in animal models of retinitis pigmentosa. *Invest Ophthalmol Vis Sci.* 2002;43:3292–3298.
17. Liang FQ, Dejneka NS, Cohen DR, et al. AAV-mediated delivery of ciliary neurotrophic factor prolongs photoreceptor survival in the rhodopsin knockout mouse. *Mol Ther.* 2001;3:241–248.
18. Faktorovich EG, Steinberg RH, Yasumura D, Matthes MT, LaVail MM. Basic fibroblast growth factor and local injury protect photoreceptors from light damage in the rat. *J Neurosci.* 1992;12:3554–3567.
19. Chow AY, Chow VY, Packo KH, Pollack JS, Peyman GA, Schuchard R. The artificial silicon retina microchip for the treatment of vision loss from retinitis pigmentosa. *Arch Ophthalmol.* 2004;122(4):460–469.
20. Pardue MT, Phillips MJ, Yin H, et al. Neuroprotective effect of subretinal implants in the RCS rat. *Invest Ophthalmol Vis Sci.* 2005;46:674–682.
21. Morimoto T, Fujikado T, Choi JS, et al. Transcorneal electrical stimulation promotes the survival of photoreceptors and preserves retinal function in Royal College of Surgeons rats. *Invest Ophthalmol Vis Sci.* 2007;48:4725–4732.
22. Morimoto T, Miyoshi T, Fujikado T, Tano Y, Fukuda Y. Electrical stimulation enhances the survival of axotomized retinal ganglion cells in vivo. *Neuroreport.* 2002;13:227–230.
23. Miller JM, Altschuler RA. Effectiveness of different electrical stimulation conditions in preservation of spiral ganglion cells following deafness. *Ann Otol Rhinol Laryngol Suppl.* 1995;166:57–60.
24. Reis DJ, Kobylarz K, Yamamoto S, Golanov EV. Brief electrical stimulation of cerebellar fastigial nucleus conditions long-lasting salvage from focal cerebral ischemia: conditioned central neurogenic neuroprotection. *Brain Res.* 1998;780:159–163.
25. Maesawa S, Kaneoke Y, Kajita Y, et al. Long-term stimulation of the subthalamic nucleus in hemiparkinsonian rats: neuroprotection of dopaminergic neurons. *J Neurosurg.* 2004;100:679–687.
26. Sato T, Fujikado T, Lee TS, Tano Y. Direct effect of electrical stimulation on induction of brain-derived neurotrophic factor from cultured retinal Muller cells. *Invest Ophthalmol Vis Sci.* 2008;49:4641–4646.
27. Sato T, Fujikado T, Morimoto T, Matsushita K, Harada T, Tano Y. Effect of electrical stimulation on IGF-1 transcription by L-type calcium channels in cultured retinal Muller cells. *Jpn J Ophthalmol.* 2008;52:217–223.
28. Sato T, Lee TS, Takamatsu F, Fujikado T. Induction of fibroblast growth factor-2 by electrical stimulation in cultured retinal Mueller cells. *Neuroreport.* 2008;19:1617–1621.
29. Pagani L, Manni L, Aloe L. Effects of electroacupuncture on retinal nerve growth factor and brain-derived neurotrophic factor expression in a rat model of retinitis pigmentosa. *Brain Res.* 2006;1092:198–206.
30. Al-Majed AA, Brushart TM, Gordon T. Electrical stimulation accelerates and increases expression of BDNF and trkB mRNA in regenerating rat femoral motoneurons. *Eur J Neurosci.* 2000;12:4381–4390.
31. Bevilacqua M, Dominguez LJ, Barrella M, Barbagallo M. Induction of vascular endothelial growth factor release by transcutaneous frequency modulated neural stimulation in diabetic polyneuropathy. *J Endocrinol Invest.* 2007;30:944–947.
32. Morimoto T, Miyoshi T, Matsuda S, Tano Y, Fujikado T, Fukuda Y. Transcorneal electrical stimulation rescues axotomized retinal ganglion cells by activating endogenous retinal IGF-1 system. *Invest Ophthalmol Vis Sci.* 2005;46:2147–2155.
33. Pardue MT, Phillips MJ, Yin H, et al. Possible sources of neuroprotection following subretinal silicon chip implantation in RCS rats. *J Neural Eng.* 2005;2:S39–S47.
34. D'Cruz PM, Yasumura D, Weir J, et al. Mutation of the receptor tyrosine kinase gene Mertk in the retinal dystrophic RCS rat. *Hum Mol Genet.* 2000;9:645–651.
35. Feng W, Yasumura D, Matthes MT, LaVail MM, Vollrath D. Mertk triggers uptake of photoreceptor outer segments during phagocytosis by cultured retinal pigment epithelial cells. *J Biol Chem.* 2002;277:17016–17022.
36. LaVail MM, Battelle BA. Influence of eye pigmentation and light deprivation on inherited retinal dystrophy in the rat. *Exp Eye Res.* 1975;21:167–192.

37. Chow AY, Pardue MT, Perlman JI, et al. Subretinal implantation of semiconductor-based photodiodes: durability of novel implant designs. *J Rehabil Res Dev.* 2002;39:313–321.
38. Chow AY, Pardue MT, Chow VY, et al. Implantation of silicon chip microphotodiode arrays into the cat subretinal space. *IEEE Trans Neural Syst Rehabil Eng.* 2001;9:86–95.
39. Nir I, Liu C, Wen R. Light treatment enhances photoreceptor survival in dystrophic retinas of Royal College of Surgeons rats. *Invest Ophthalmol Vis Sci.* 1999;40:2383–2390.
40. Ball SL, Pardue MT, Chow AY, Chow VY, Peachey NS. Subretinal implantation of photodiodes in rodent models of photoreceptor degeneration. In: Hollyfield JG, Anderson RE, LaVail MM, eds. *IX International Symposium on Retinal Degeneration.* New York: Kluwer/Plenum Press; 2001:175–180.
41. Sagdullaev BT, DeMarco PJ, McCall MA. Improved contact lens electrode for corneal ERG recordings in mice. *Doc Ophthalmol.* 2004;108:181–184.
42. Rozen S, Skaletsky H. Primer3 on the WWW for general users and for biologist programmers. *Methods Mol Biol.* 2000;132:365–386.
43. Livak KJ, Schmittgen TD. Analysis of relative gene expression data using real-time quantitative PCR and the 2(-ΔΔC(T)) method. *Methods.* 2001;25:402–408.
44. DeMarco PJ Jr, Yarbrough GL, Yee CW, et al. Stimulation via a subretinally placed prosthetic elicits central activity and induces a trophic effect on visual responses. *Invest Ophthalmol Vis Sci.* 2007;48:916–926.
45. Morimoto T, Choi J, Miyoshi T, Fukuda Y, Tano Y, Fujikado T. Effects of transcorneal electrical stimulation on the survival of photoreceptors in Royal College Surgeons rats. *Invest Ophthalmol Vis Sci.* 2005;46:183.
46. Cao W, Li F, Steinberg RH, LaVail MM. Development of normal and injury-induced gene expression of aFGF, bFGF, CNTF, BDNF, GFAP and IGF-I in the rat retina. *Exp Eye Res.* 2001;72:591–604.
47. Wen R, Song Y, Cheng T, et al. Injury-induced upregulation of bFGF and CNTF mRNAS in the rat retina. *J Neurosci.* 1995;15:7377–7385.
48. Yamazaki H, Ohguro H, Maeda T, et al. Preservation of retinal morphology and functions in royal college surgeons rat by nilvadipine, a Ca(2+) antagonist. *Invest Ophthalmol Vis Sci.* 2002;43:919–926.
49. Tao W. Application of encapsulated cell technology for retinal degenerative diseases. *Expert Opin Biol Ther.* 2006;6:717–726.
50. Sieving PA, Caruso RC, Tao W, et al. Ciliary neurotrophic factor (CNTF) for human retinal degeneration: phase I trial of CNTF delivered by encapsulated cell intraocular implants. *Proc Natl Acad Sci U S A.* 2006;103:3896–3901.

RETRACTION

"Effect of Superposed Electromagnetic Noise on DNA Damage of Lens Epithelial Cells Induced by Microwave Radiation,"

Yao K, Wu W, Yu Y, Zeng Q, He J, Lu D, Wang K. *Invest Ophthalmol Vis Sci.* 2008;49(5):2009–2015.
DOI: 10.1167/iovs.07-1333. PMID: 18436834.

An investigation by the Editor-in-Chief, Paul L Kaufman, *IOVS*, found that this paper was previously published.

It is against the policy of the Association for Research in Vision and Ophthalmology (ARVO) to consider any paper or component of a paper that has been published or is under consideration for publication elsewhere.

The paper is therefore being retracted by ARVO from the *IOVS* journal.